IEEE Access
Multidisciplinary | Rapid Review | Open Access Journal

Received December 26, 2019, accepted January 6, 2020, date of publication January 10, 2020, date of current version January 21, 2020.

Digital Object Identifier 10.1109/ACCESS.2020.2965768

Machine-Learning Algorithms for Mapping Debris-Covered Glaciers: The Hunza Basin Case Study

AFTAB AHMED KHAN[1], AKHTAR JAMIL[2], DOSTDAR HUSSAIN[1], MURTAZA TAJ[3], GUL JABEEN[1], AND MUHAMMAD KAMRAN MALIK[4]

[1]Department of Computer Sciences, Karakoram International University, Gilgit 15100, Pakistan
[2]Department of Computer Engineering, Istanbul Sabahattin Zaim University, 34303 Istanbul, Turkey
[3]Department of Computer Science, Lahore University of Management Sciences (LUMS), Lahore 54792, Pakistan
[4]Punjab University College of Information Technology (PUCIT), Punjab University, Lahore 54590, Pakistan

Corresponding author: Aftab Ahmed Khan (aftab.ahmed@kiu.edu.pk)

ABSTRACT Global warming is one of the main challenges of recent times. The glaciers are melting faster than expected which has resulted in global mean sea level rise and increased the risk of floods. The development of modern remote sensing technology has made it possible to obtain images more frequently than ever before. On the other side, the availability of high-performance computing hardware and processing techniques have made it possible to provide a cost-effective solution to monitor the temporal changes of glaciers at a large scale. In this study, supervised machine learning methods are investigated for automatic classification of glacier covers from multi-temporal Sentinel-2 imagery using texture, topographic, and spectral data. Three most commonly used supervised machine learning techniques were investigated: support vector machine (SVM), artificial neural network (ANN) and random forest (RF). The proposed method was employed on the data obtained from Passu watershed in Hunza Basin located along the Hunza river in Pakistan. Three main classes were considered: glaciers, debris-covered glaciers and non-glaciated areas. The data was split into training (70%) and testing datasets (30%). Finally, an area-based accuracy assessment was performed by comparing the results obtained for each classifier with the reference data. Experiments showed that the results produced for all classifiers were highly accurate and visually more consistent with the depiction of glacier cover types. For all experiments, random forest performed the best (Kappa = 0.95, f-measure = 95.06%) on all three classes compared to ANN (Kappa = 0.92, f-measure = 92.05) and SVM (Kappa = 0.89, f-measure = 91.86% on average). The high classification accuracy obtained to distinguished debris-covered glaciers using our approach will be useful to determine the actual available water resources which can be further helpful for hazard and water resource management.

INDEX TERMS Artificial neural network (ANN), glacier mapping and remote sensing, random forest (RF), support vector machine (SVM).

I. INTRODUCTION

The Karakoram range and its surroundings are the most heavily glaciated area of the world outside the polar region spanning the borders of China, India, Pakistan, Tajikistan, and Afghanistan [1]. The range consists of several highest peaks (e.g., K2 and Gasherbrum-I) and largest glaciers (e.g., Siachen and Biafo glaciers) [2]. These large glaciers are very sensitive to climatic changes and any radical change may result in floods or drought which will have a high impact on the downstream population in terms of their agricultural, livelihood and living [3]. Moreover, urbanization in downstream cities is expanding day-by-day [4]. Therefore, it is imperative to monitor glaciers continuously to determine and understand the dynamics of glaciers' sensitiveness to climate changes.

In the past, glaciers mapping was done usually through field surveys. However, it was very problematic in difficult terrains and inaccessible areas [5]. Nowadays, monitoring and mapping of glaciers are carried out through satellite

The associate editor coordinating the review of this manuscript and approving it for publication was Lefei Zhang.

remote sensed data which are more efficient, cheaper and provide ways to derive several important properties of glaciers such as coverage, snow depth, time span, etc. [6].

In recent decades, several researchers have used different methods to monitor changes in glacier-covered areas and ice for specific periods. Those methods include segmentation through visual interpretation and band ratios or band indices of remotely sensed images [7]–[9]. Furthermore, supervised algorithms, unsupervised algorithms, and decision tree-based methods are also proposed to derive such information [10]. Similarly, the debris-covered glaciers are classified using band ratios and manual onscreen digitalization [11]. Also, several researchers proposed semiautomatic methods for classification and more recently Unmanned Aerial Vehicles (UAVs) are used for mapping glaciers with higher accuracy [12].

However, spatial diversity/variety of glacier data is a big hurdle in classification as it makes the process of understanding and monitoring the glacier changes even more challenging. Moreover, mapping of glaciers using remotely sensed data is not a trivial task due to various factors such as the presence of clouds over the mountainous areas, spectral similarity of glaciers covered with debris and adjacent rocks/areas. Nevertheless, in recent decades there is an improvement in accuracy of mapping debris-covered glaciers using field measurements, land surface temperature, utilizing multispectral band ratios, and texture information within an image [13]. However, these traditional approaches and methods of measurements and classification needs an immediate improvement to monitor and to determine the actual status of water resources i.e., glaciers in terms of expansion or retreat to manage drought and floods in downstream population.

Glacier inventories for the Karakoram region are developed by several sources that include source [14], International Center for Integrated Mountain Development (ICIMOD), and World Glacier Inventory using different approaches by utilizing remotely sensed data. However, they have limitations of having only outlines of naked ice glaciers and are less accurate for debris-covered glaciers. Debris-covered glaciers play a very important role in the glacier mass balance and controlling the ice melting. Thin debris cover increases the ice melting rate while thick debris cover reduces the melting rate. Therefore, it is important to assess, and map debris-covered glaciers to determine its effects on ice ablation and glacier response in terms of variations in mass balance and as an indicator for climatic change.

Hunza basin in the North western Karakoram is one of the sensitive regions in the world where a minor change in climatic conditions may result in drastic glacier consequences [15], [16]. Most of the researchers in this basin have focused on debris-free glaciers and few studies have mapped debris-covered glaciers by manual on-screen digitalization [17], [18]. However, the accuracy of manual digitalization of debris-covered glaciers varies based on the resolution of image and expertise of person resulting in different mappings for the same glacier. This problem of accuracy needs to be addressed.

Machine learning (ML) approaches have proven to be very effective for classification of remote sensing (RS) data by extracting and selection of feature for hyperspectral images [19], [20]. ML methods have produced significantly promising results in many RS applications, such as tree delineation [21], land cover classification [22], buildings and tree species extraction [23], [24], fault diagnosis [25] and fault-tolerant control [26]. In the context of glaciers, ML techniques have also been used for mapping on large glaciers from RS data. For instance, [27] has employed RF classifier for automatic classification of ice cover types from Landsat-8 imagery and multiple digital elevation model (DEM) data. Similarly, source [28] has implemented SVM for forecasting of snow avalanches from temporal data obtained from satellite imagery. Reference [24] has proposed a method for change detection of Arctic glaciers obtained from multi-temporal multi-polarization synthetic aperture radar images. In addition, some recent studies have presented efficient approaches to classify glacier data using ML methods such as RF from multispectral images [29].

In this research work, we investigated three supervised ML classifiers for classification of the glaciers, debris-covered glaciers and non-glaciated areas from remotely sensed data. Several discriminative features were derived from the data that include spectral, textural and topographic features to train and test the models. The main objective of this paper is to assess the performance of the ML algorithms for their classification of the glacier areas particularly debris-covered glaciers which are very similar to the adjacent barren land. Because of this similarity most of the supervised and unsupervised classification algorithms in the past have less accuracy resulting in under or over estimation of water resources i.e. glaciers. Based on the assessment of three classifiers we will be able to determine the actual status of water resources with high accuracy that will help to relevant authorities (including government) and researchers to make crucial decisions.

The rest of the paper is organized as follows. First, the study area and the used datasets are presented. Second, classification methods are described which is followed by application of proposed methods in the study area. Finally, an assessment and comparison of the results are carried out. Further, the paper is completed with concluding remarks.

II. STUDY AREA

The study area is Passu watershed in Hunza basin located along the Hunza River at the south of the tongue of the Batura glacier, extends between longitude 74.20 and latitude 36.30 degrees (Figure 1). The elevation ranges from 3000 m to 8000 m. The selected area's land cover consists of snow, debris-free glaciers, debris-covered glaciers, barren land, vegetation, and water.

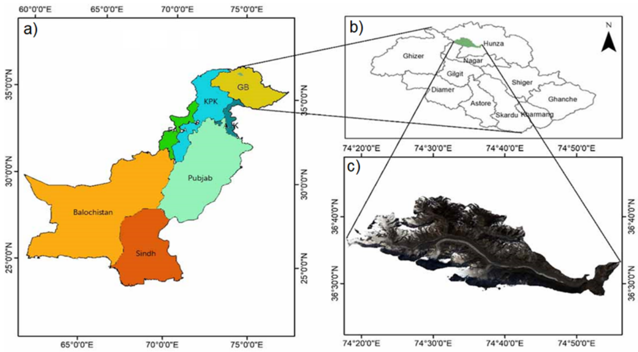

FIGURE 1. **a) Map of Pakistan and location of GB b) main districts of GB c) Selected study area.**

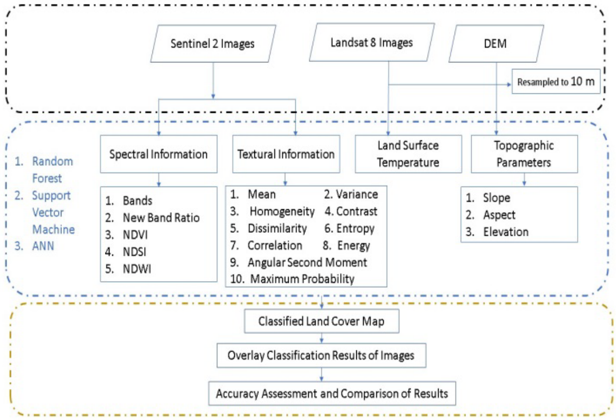

FIGURE 2. **Flowchart of methodology to classify images into glaciers, debris-covered glaciers, and non-glacier area using three machine learning algorithms.**

III. MATERIAL

A. LANDSAT AND SENTINEL DATA

The Sentinel-2 and Landsat-8 images of the study area were acquired from the website of Google Earth Engine (GEE) provided by United States Geological Survey (USGS) with cloud coverage of less than 20% in the year 2018 from 15 August to 15 October (Image without clouds and mean value) with images' spatial resolution of 10 meters and 30 meters, respectively. The selection of these dates is at the end of the ablation period to avoid seasonal snow cover to map the actual glaciers. The images we used were already corrected and converted from raw digital numbers (DNs) to the top of atmosphere (TOA) radiance utilizing radiometric parameters by GEE. Further, we used images from GEE which have already been corrected for atmospheric correction using the Second Simulation of the Satellite Signal in the Solar Spectrum model [30]. The Landsat-8 imagery was resampled to 10 m resolution to make it comfortable with the sentinel-2 dataset to utilize thermal data from band-10.

B. DEM AND BOUNDARY DATA

Global Digital Elevation Model (GDEM) data of Shuttle Radar Topography Mission (SRTM) was used to provide topographic information whose data has been void-filled using open-source data of Advanced Spaceborne Thermal Emission and Reflection Radiometer (ASTER) Global Digital Elevation (GDEM version 2) [31]. The data was downloaded from GEE platform in GeoTIFF format. This data is provided by NASA JPL at a resolution of 30 meter with a vertical accuracy of 15 m. The GDEM's resolution was resampled to make it consistent with the spatial resolution of the Sentinel imagery. The boundary data of the study area was developed by authors whereas basin and administrative boundaries data were collected from government official sources.

C. GLACIER INVENTORIES

The reference data for our selected area was manually delineated by visually inspecting the classes of interest. In addition, two other glacier inventories were also used from two different sources for comparison which include inventories developed by ICIMOD [32], [33], and source [13]. These inventories are developed based on the remote sensing data that were captured in 2000 and 2013. All datasets were projected to the same coordinate system of the 1984 World Geodetic System (WGS 84) with Universal Transverse Mercator (UTM) Zone 43 North.

IV. METHODOLOGY

The overall workflow of the proposed method is shown in Figure 2. We implemented our method in three steps. First, a set of features were extracted, which include spectral, textural and topographic features. The spectral features include reflectance information from each band, Normalized Difference Vegetation Index (NDVI), Normalized Difference Snow Index (NDSI), Normalized Difference Water Index (NDWI), and New Band Ratio (NBR) [10]. The textural features were derived from the grey level co-occurrence matrix which was generated by a moving window of size 3 x 3. These features include mean, variance, homogeneity, contrast, dissimilarity, entropy, energy, correlation and angular second momentum. The topographic features were obtained from DEM which include slope, aspect and evaluation information. In addition to these three features, land surface temperature from band-10 of Landsat-8 imagery was also included and combined all these features into 1 x N dimensional vector for each pixel. Where N is the dimension of the feature vector which was 74 in our case.

In the second step, three commonly used machine learning classifiers (SVM, RF, and ANN) were trained and tested on our data. The feature vectors obtained in the previous step were fed into each classifier which produced classification maps for each class, i.e. glaciers, debris-covered glaciers and non-glacier areas.

In the last step, an area-based accuracy assessment was performed by comparing the produced output with the reference data to evaluate the performance of the proposed method for each classifier. To further quantify, the results were expressed in terms of precision, recall and f-measure.

A. FEATURE EXTRACTION

Three types of features were extracted which include spectral, topographic, and textural features. The following sections describe the process for extraction of each type of feature.

1) SPECTRAL FEATURES

The spectral features were derived directly for the available six bands of the Sentinel images which include Green, Blue, Red, Near Infrared, Shortwave Infrared 1, and Shortwave infrared 2. In addition, land surface temperature was obtained from thermal infrared-1 band (B10 band) of Landsat 8, and several indices were derived from various combination of these bands. Spectral indices extracted were Normalized Difference Vegetation Index (NDVI), Normalized Difference Water Index (NDWI), Normalized Difference Snow Index (NDSI) and NBR [11]. Following formula were used to calculate these indices:

$$\text{NDVI} = \frac{(\text{Near Infrared} - \text{Red})}{(\text{Near Infrared} + \text{Red})}$$

$$\text{NDWI} = \frac{(\text{Green} - \text{Nearinfrared})}{(\text{Green} + \text{Nearinfrared})}$$

$$\text{NDSI} = \frac{(\text{Green} - \text{Shortwave infrared 1})}{(\text{Green} + \text{Shortwave infrared 1})}$$

$$\text{NBR} = \frac{\text{Shortwave infrared}}{(\text{Red} / \text{Nearinfrared})}$$

The NDVI is calculated using red and near-infrared bands, NDWI is calculated from green and near-infrared bands while green and short wave near infrared-1 bands are used to calculate NDSI. NDVI is useful to determine the vegetation areas, NDWI helps to identify water bodies and NDSI give important clue about the presence of glacier in the image. Further, NBR is computed using the formula given above from source [11]. The purpose of using this ratio is to determine its influence in the decision of the glaciated area and it may assist to detect debris-covered glaciers.

2) TOPOGRAPHIC FEATURES

The topographic features are extracted from DEM which include elevation, slope, and aspect. Elevation represents the height above the sea level, slope represents horizontal plane, and aspect represents angle to the north (up) and is calculated with the convention of 0 degrees angles increasing clockwise.

3) TEXTURAL FEATURES

Since texture features cannot be directly derived from reflectance information, therefore, first a GLCM [34] was constructed by scanning the whole image using a small window of size 3 x 3 and then several textural features were derived from it. These features include entropy, second moment, mean, dissimilarity, variance, energy, homogeneity, correlation, and contrast, for each spectral band (Blue, Green, Red, NIR, SWIR1, and SWIR2 band). These values were computed using the GLCM [34]. The formula for the computation of these features is given by [35]. We used open-source SNAP tool from the European Space Agency to compute these features [36].

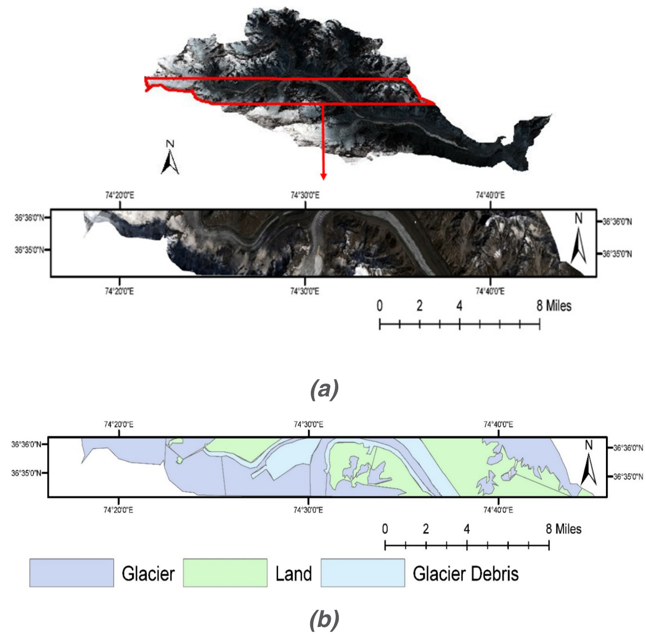

FIGURE 3. **(a). The focused area of study, from where the training and test dataset were extracted. (b). The reference image for the study areas showing three classes: glaciers, debris-covered glacier and non-glacier areas.**

B. ANALYSIS OF FEATURES

The extracted features were further analyzed to determine their discrimination power for the classification of input data into the classes as highly discriminative features are required to obtained high classification accuracy for machine learning classifiers. Figure 4 shows the spectral reflectance information captured by different bands of Sentinel 2 imagery. As we can see that the reflectance information of the glacier, debris-covered glaciers and land cover overlap with each other. This indicates that using only the reflectance information for each class may not be able to distinguish the classes. Therefore, extraction of some other useful feature using the reflectance information is useful. Moreover, the reflectance of land cover classes spans over a large range due to the presence of various types of land cover (bare land, vegetation, water body etc.).

In addition, glacier and debris-covered glaciers have very similar reflectance making it very difficult to decide or classify based on surface reflectance only. Here, NDSI plays a key role as based on a certain threshold it can easily distinguish snow/glacier from other classes. Similarly, NDVI plays a key role to classify vegetation areas and NDWI plays the main part to determine about water bodies. Thus, these indices are very supportive to determine non-glacier and glacier area classes.

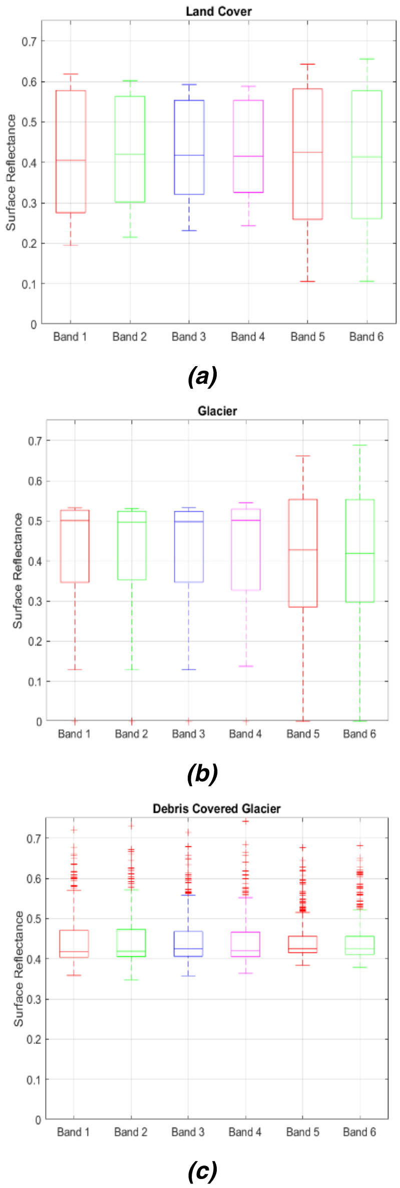

FIGURE 4. **Surface reflectance information for (a) land (non-glacier areas), (b) glacier, and (c) debris-covered glaciated areas.**

FIGURE 5. **Two points (A and B) and a line to observe change in land surface temperature with respect to elevation.**

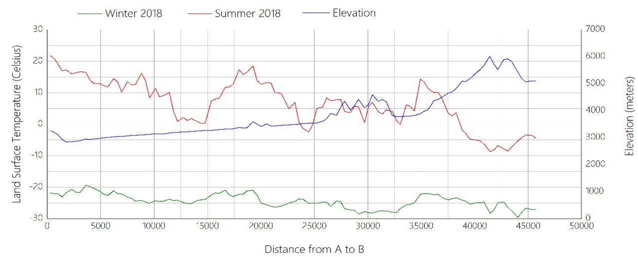

FIGURE 6. **Change in LST in winter and summer with the change in elevation between two points 'A' and 'B'.**

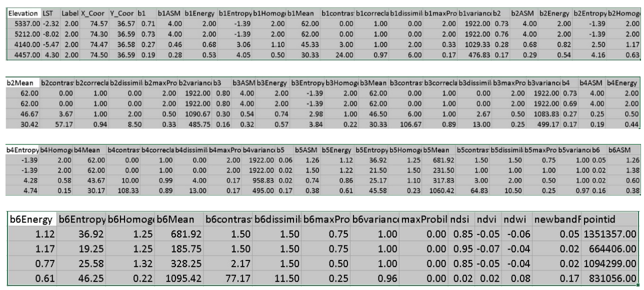

Elevation	LST	Label	X_Coor	Y_Coor	b1	b1ASM	b1Energy	b1Entropy	b1Homog	b1Mean	b1contras	b1correla	b1dissimil	b1maxPro	b1varianc	b2	b2ASM	b2Energy	b2Entropy	b2Homog
5337.00	-2.32	2.00	74.57	36.57	0.71	4.00	2.00	-1.39	2.00	62.00	0.00	1.00	0.00	2.00	1922.00	0.73	4.00	2.00	-1.39	2.00
5212.00	-8.02	2.00	74.30	36.59	0.73	4.00	2.00	-1.39	2.00	62.00	0.00	1.00	0.00	2.00	1922.00	0.76	4.00	2.00	-1.39	2.00
4140.00	-5.47	2.00	74.47	36.58	0.27	0.46	0.68	3.06	1.10	45.33	3.00	1.00	2.00	0.33	1029.33	0.28	0.68	0.82	2.50	1.17
4457.00	4.30	2.00	74.50	36.59	0.19	0.28	0.53	4.05	0.50	30.33	24.00	0.97	6.00	0.17	476.83	0.17	0.29	0.54	4.16	0.63

b2Mean	b2contras	b2correla	b2dissimil	b2maxPro	b2varianc	b3	b3ASM	b3Energy	b3Entropy	b3Homog	b3Mean	b3contras	b3correla	b3dissimil	b3maxPro	b3varianc	b4	b4ASM	b4Energy
62.00	0.00	1.00	0.00	2.00	1922.00	0.80	4.00	2.00	-1.39	2.00	62.00	0.00	1.00	0.00	2.00	1922.00	0.73	4.00	2.00
62.00	0.00	1.00	0.00	2.00	1922.00	0.80	4.00	2.00	-1.39	2.00	62.00	0.00	1.00	0.00	2.00	1922.00	0.69	4.00	2.00
46.67	3.67	1.00	2.00	0.50	1090.67	0.30	0.54	0.74	2.98	1.00	46.50	6.00	1.00	2.67	0.50	1083.83	0.27	0.25	0.50
30.42	57.17	0.94	8.50	0.33	485.75	0.16	0.32	0.57	3.84	0.22	30.33	106.67	0.89	13.00	0.25	499.17	0.17	0.19	0.44

b4Entropy	b4Homog	b4Mean	b4contras	b4correla	b4dissimil	b4maxPro	b4varianc	b5	b5ASM	b5Energy	b5Entropy	b5Homog	b5Mean	b5contras	b5dissimil	b5maxPro	b5varianc	b6	b6ASM
-1.39	2.00	62.00	0.00	1.00	0.00	2.00	1922.00	0.06	1.26	1.12	36.92	1.25	681.92	1.50	1.50	0.75	1.00	0.05	1.26
-1.39	2.00	62.00	0.00	1.00	0.00	2.00	1922.00	0.02	1.50	1.22	21.50	1.50	231.50	1.00	1.00	1.00	1.00	0.02	1.38
4.28	0.58	43.67	10.00	0.99	4.00	0.17	958.83	0.02	0.74	0.86	25.17	1.10	317.83	3.00	2.00	0.50	1.00	0.02	0.60
4.74	0.15	30.17	108.33	0.89	13.00	0.17	495.00	0.17	0.38	0.61	45.58	0.23	1060.42	64.83	10.50	0.25	0.97	0.16	0.38

b6Energy	b6Entropy	b6Homog	b6Mean	b6contras	b6dissimil	b6maxPro	b6varianc	maxProbil	ndsi	ndvi	ndwi	newbandF	pointid
1.12	36.92	1.25	681.92	1.50	1.50	0.75	1.00	0.00	0.85	-0.05	-0.06	0.05	1351357.00
1.17	19.25	1.25	185.75	1.50	1.50	0.75	1.00	0.00	0.95	-0.07	-0.04	0.02	664406.00
0.77	25.58	1.32	328.25	2.17	1.50	0.50	1.00	0.00	0.85	-0.05	-0.04	0.02	1094299.00
0.61	46.25	0.22	1095.42	77.17	11.50	0.25	0.96	0.00	0.02	0.02	0.08	0.17	831056.00

FIGURE 7. **Snap shot of the first five rows (five points) with their corresponding column names from dataset.**

It was also observed that the debris-covered glaciers and surrounding bare land had similar surface reflectance, making it challenging for the classifier to decide about its class. In this case, the land surface temperature feature is helpful to decide as supraglacial debris have always low temperature than the surrounding bare land. In addition, elevation also provides useful information about the presence of glaciers. In our dataset, all the glaciers are located more than 2500 m elevation. Therefore, a glacier class identified lower than 2500 m elevation will be determined as an outliner and be reassessed for its classification. To show the difference of land surface temperature with respect to elevation and debris-covered glaciers we took two points 'A' and 'B' from our sample dataset and analyzed land surface temperature for summers and winters in comparison with elevation shown in Figure 5 and Figure 6. The figures clearly show that supraglacial debris and ice with debris have low land surface temperatures (less than zero Celsius) in summer. Whereas, in winters the temperature remains almost the same in the whole area which is less than -20 Celsius. Therefore, with the support of land surface temperature information based on the assumption that debris-covered glaciers will remain stable in low slope and aspect areas can be differentiated as glaciers and non-glaciers.

Total 74 features were derived from the input images which include spectral features (six bands, land surface temperature, NBR, and NDVI, NDSI, NDWI), textural feature (10 features for each of 6 bands, in total 60 features), and topography features (elevation, slope, and aspect). A snap shot of the first five rows with their corresponding column name of the dataset is given in Figure 7.

C. CLASSIFICATIONS

1) RANDOM FOREST (RF) CLASSIFICATION

RF is an ensemble classifier that can be used for both regression and classification tasks. It consists of a set of individual decision trees (DT) which are created from a subset of training samples drawn randomly with replacement. The selected samples, known as in-bag samples, are used to train the trees while the remaining samples, known as Out-of-Bag (OOB) samples, are used for cross-validation to estimate how well the model performed. This random selection of input training samples helps to overcome the overfitting problem of the training dataset. In general, two- third of the training samples are selected to train the model while remaining ones are used for cross-validation [37]. The user defines the number of decision trees (N) to be used to construct the RF classifier and the number of features (M) to be used to split the data at each node. Generally, M is a subset of the whole feature set which helps to de-correlate the individual trees. Once the user sets both M and N, the RF classifier randomly grows the forest up to N. The final decision about a test sample is taken by averaging the resulting probabilities of individual trees. It means, the test data is evaluated by each tree in the ensemble and its membership decision is based on the maximum voting of the trees for a particular class. A detailed description of the application of RF for remote sensing data can be found in [37].

2) SUPPORT VECTOR MACHINE (SVM) CLASSIFICATION

SVM is a non-parametric classifier, which is primarily designed to solve binary classification problems. However, it can be adopted to multiclass classification tasks by constructing multiple binary classifiers. It uses strategies like one-against-one or one-against-all and then a voting mechanism is used to distinguish the members of one class from others. The main objective is to determine a linear discriminant function that maximizes the margin of separation between each class [38]. However, in many cases, the data may not be linearly separable. To cope with this problem, SVM transforms the data into a higher-dimensional space by applying a kernel function. It then fits the optimum hyperplane in the transformed space to distinguish between classes of interest by applying an optimization function. The most commonly used kernel functions include linear, polynomial and radial basis function (RBF). In this study, we selected RBF kernel, as it is computationally efficient and easy to implement. A detailed description about SVM classifier can be found in [39].

3) ANN CLASSIFICATION

Like SVM, ANN is also a nonparametric classification technique. The computational complexity to train ANN is relatively higher, but it can learn to classify complex nonlinearly separable data with high accuracy [40]. Various Models of ANN have been proposed such as RBF, backpropagation, multilayer perceptron (MLP) etc. Among all, MLP is the most commonly used model for various pattern recognition tasks. It consists of a set of input, hidden (one or more) and output layers. The neurons on the hidden and output layer produce their activation by applying nonlinear activation function. Usually, gradient-based learning algorithms are applied to train the ANN model, which is generally slow but may easily converge to a local-minima.

V. EXPERIMENTAL RESULTS

The effectiveness of the proposed method for classification of glaciers, debris-covered glaciers and non-glaciated cover types were evaluated by calculating overall accuracy and Kappa coefficient for each classifier. Supervised classifiers need both data and labels for training. Therefore, we manually selected training samples for each class of interest. In addition, supervised machine learning methods depend on many parameters, we employed grid search technique to find the optimal parameters for each classifier. The obtained optimal parameters were used to train the model and then test data was classified into corresponding classes. The following sections describe the implementation details.

A. TRAINING SAMPLE SELECTION

Since supervised classification algorithms require training samples from all possible classes, therefore, the training samples were collected for the three land cover types: glaciers, glacier with debris and non-glaciated (Barren land, vegetation, water, and agriculture land) areas. We selected a specific area of interest shown in Figure 3 (a) that contains all three classes i.e., glaciers, debris-covered glaciers, and non-glaciated areas. In total, we collected 26,88723 pixels, of which 391907 were labeled as a glacier with debris, 1354622 as glacier, and 942194 as non-glaciated areas. The collected dataset was further split into two sets: training (70%) and testing (30%). In total 1882106 pixels and 806616 pixels were used for training and testing, respectively. The training samples selected in such a way that they were geographically scattered over the whole study area and ensured representation from each class with the same percentage of samples of each three classes using the stratified sampling technique to avoid bias towards any particular class.

B. FINE-TUNING MODEL PARAMETERS

To build the ML models, several adjustable parameters need to be examined. The proper choice of the parameters of the classifier is crucial to avoid overfitting and produce a model with good classification accuracy [28]. Therefore, these parameters need fine-tuning to obtain their optimal values. We employed k-fold cross-validation to create and optimize models for all three ML algorithms (SVM, ANN, RF). Optimal values for parameters were obtained by cross-validation on the original training data set. Finally, the set of parameters for which model produced optimal results were selected for testing the model. Specific details of parameter tuning using grid-search for each classifier is described below.

Performing parameter optimization using manual methods can be very time consuming especially when the learning algorithm has many parameters. In this study, we employed grid-search method, which is basically an exhaustive search strategy to obtain an optimal set of parameters from the hyper-parameter space. The following sections provide specific details of parameter tuning using grid-search for each classifier.

1) SVM MODEL PARAMETER SELECTION

To apply the linear SVM model on nonlinearly separable data, we first transform each instance of the data into a higher-dimensional space using a kernel function. One of the most commonly used kernel functions is RBF kernel. Two data points x_i and x_j can be transformed using RBF kernel with the following equation

$$K(x_i, x_j) = exp(-\gamma ||x_i - x_j||^2)$$

where γ is gamma, which represents the kernel width. This kernel requires turning of only one parameter γ. So, the SVM classifier with RBF kernel requires tuning of total two important petameters: cost (C), which is used to standardizing the error of misclassification and γ. Higher values of C mean larger penalties for misclassification, which may result in overfitting of data, whereas larger values of γ affects the shape of the decision boundary.

To choose the optimal values for C and γ using k-fold cross-validation (CV), the data is split into k subsets ($k = 10$). One subset is used as testing data while remaining k-1 training subsets are used for training. The CV error is calculated for the SVM classifier using various combinations of C and γ. Finally, we select the parameter combination which produced the best cross-validation accuracy to train the SVM on the whole training dataset.

Since, there is no common rule to define exact ranges of C and γ for searching the best combination. Therefore, in our experiment we decided to search the parameter C in the range $= [e^{-5}, e^{-3}, \ldots e^{9}]$, while $\gamma = [e, e^{-7}, \ldots, e^{3}]$. The optimal values selected for C and γ were e^3 and e^{-2} respectively.

2) ANN MODEL PARAMETER SELECTION

Since, ANN classifier has a relatively larger number of parameters to fine-tune, we selected only momentum and learning rate. Other parameters were set to a fixed value such as, the number of iterations = 1000, sigmoid as activation function, and empirically calculated the number of hidden neurons to be 200 in the hidden layer. The learning rate was searched between 0.001 and 0.5 while momentum between 0 and 0.9. The values that produced optimal accuracy were 0.1 and 0.8 for learning rate and momentum respectively.

3) RF MODEL PARAMETER SELECTION

As mentioned before, RF classifier model construction requires two parameters: the number of decision trees (N) and the number of variables used to split data (M). Generally, N has little impact on the classification accuracy of the classifier. Since increasing the value of N does not overfit RF classifier, it can be as large as possible. However, increasing the value of M may increase the computational time of the RF classifier. The value of N was searched in the range 50-500 with a step size of 50. Finally, 250 was selected as the optimal value. For the value of M, the literature shows that it is determined usually by taking the square root of the number of input variables [41]. Since we used 74 input features therefore, the value of M was set to 8.

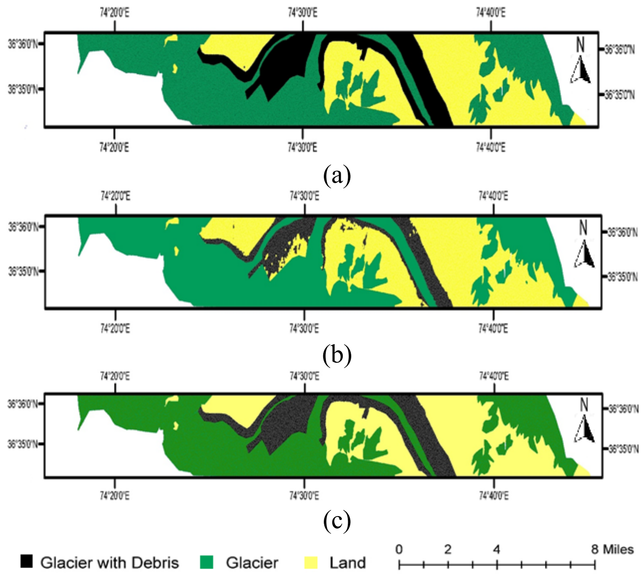

FIGURE 8. Classification of our selected sample area. a) classification by RF (b) classification by ANN (c) classification by SVM.

4) CLASSIFICATION RESULTS AND POST PROCESSING

After selecting the optimal parameters and training the models, the same set of features (74 features) were derived from the test data and fed into the trained classifiers. Each classifier produced a classification map by assigning the pixels a class label for one of the three classes. The unclassified pixels were assigned to the background class. For better interpretation, the obtained results were labelled with different colors as shown in Figure 8. Visual analysis and inspection of results of each algorithm shown in Figure 8 can be interpreted as all the algorithms have classified all three classes with high accuracy. Although there were some issues (misclassify) in classifying glaciers with debris and non-glacier areas.

Before performing the final accuracy assessment, a post-processing step was performed on the classification results obtained from each classifier to reduce some unwanted outputs and to increase the classification accuracy. Since the study area was dominated by the glacier, the classification maps produced by each classifier consisted of objects relatively larger in size. Therefore, it was imperative to remove small isolated objects and holes present in the objects of interest. To overcome these issues, we applied morphological

TABLE 1. Accuracy assessment of three algorithms for classification of glacier, Debris-covered glacier and land.

Classifier	Cover Type	Precision (%)	Recall (%)	F-Measure (%)	Kappa
ANN	Glacier	93.00	93.00	93.00	0.93
	Debris-covered Glacier	92.05	92.02	92.00	0.92
	Land	92.98	92.19	92.58	0.92
SVM	Glacier	91.98	91.98	91.98	0.89
	Debris-covered Glacier	90.47	89.32	89.89	0.89
	Land	91.56	91.06	91.81	0.91
RF	Glacier	96.76	96.76	96.76	0.96
	Debris-covered Glacier	95.06	95.06	95.06	0.95
	Land	ss95.65	95.65	95.65	0.95

opening with a structuring element of size 5 x 5 to remove small objects and holes present in the objects. Moreover, geometrical constraints were applied to the connected components of the output image to further remove the noisy elements missed by the morphological opening step. The end result consisted of cleaner glacier objects (both debris-covered and glacier) and non-glacier objects.

C. ACCURACY ASSESSMENT

The effectiveness of the proposed method was evaluated in terms of overall accuracy (OA), precision (P), recall (R) and Kappa Coefficient (K). An area-based quantitative comparison was performed between the obtained results and the reference data. The total sample area selected for accuracy assessment was 142 km^2 with 806,616 pixels. For the selected area the reference data was prepared manually by delineating the three classes by experts. In addition, we compared our results with ICIMOD glacier inventory datasets [33] as well as the source [14].

The classification accuracy obtained for the three selected supervised classifiers is summarized in Table 1. The overall accuracy (OA) is 92.77 % and overall Kappa is 0.92 which indicates good classification results for the three classes. The f-measure for the glacier class is 91.00 %, 93.98 % and 96.76 % for ANN, SVM and RF classifier respectively. Similarly, for the glacier with debris class the same classifiers produced 92.58 %, 89.89 % and 95.06 % respectively. The classification accuracy for non-glacier area class for the same classifiers were 92.58 %, 91.81 % and 95.65 % respectively.

Although all three classifiers produced good classification accuracy, however, RF produced the highest classification accuracy for all three classes compared to SVM and ANN. SVM classifier produced least overall accuracy on our dataset. Especially, for the glacier and glacier with debris classes there were more miss classifications for SVM and ANN classifiers. This could be ascribed to the fact that there were high spectral similarities between the classes specifically along the border.

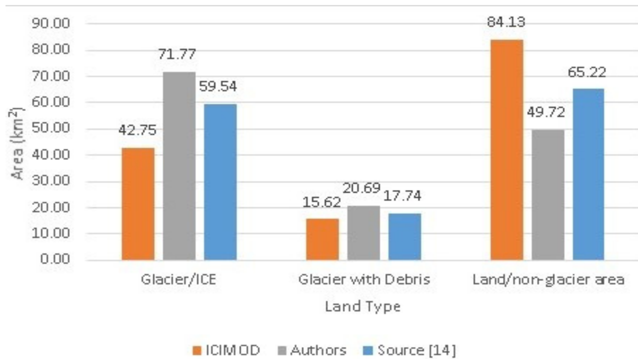

FIGURE 9. Comparison of referenced datasets with their classes.

The referenced datasets have different classifications with minor differences i.e., inventory developed by ICIMOD contains 42.72 % glacier, [14]'s inventory contains 59.5 %, and our own classification of the area contains 71 % of glacier area of the total area in our selected sample area as shown in Figures 9. The inventory developed by source [14] and ICIMOD is based on the imagery of 30 m resolution and almost 7 to 15 years old. Whereas in our case we used sentinel-2 images with 10 m resolution and validated our results with google earth images. Our highly accurate (accuracy of 90%) classification model can be very helpful to avoid these discrepancies (Figure 9) in different classifications by several producers.

Visually we can also see from the Figures 8 (a, b, c) that the classification results for all three classifies showed good coherence in the whole study area. However, there was some confusion between glacier and glacier with debris in some regions. It may be very difficult to find the differences between the two classes due to spectral similarity. Also, there were some inconsistencies in some areas due to clouds in the images. Although we selected the images with minimum clouds, however, their presence also resulted in some miss-classifications.

VI. CONCLUSION

In this paper, the results presented show the benefits of using ML approaches to classify the glacier surfaces covered with and without debris as well as usage of remote sensing data. We used the freely available multi-temporal Sentinel-2 data. Passu (Hunza basin) was selected as the study area, which is in the northern region of Pakistan in the Karakoram range. Three most commonly used ML classifiers, i.e., SVM, ANN and RF, were selected. To achieve our goals, three classes of interest were defined: glacier, debris-covered glacier, and non-glacier areas. A whole region was selected to obtain the training samples for each class and then a set of spectral, textural and topographical features were extracted. All three types of features were combined into a single vector and fed into each classifier individually for classification. The classifiers produced classification maps for glacier cover which were then compared with the reference data. The results indicated that RF was relatively more effective compared to SVM and ANN. The statistical results were more consistent when compared with the reference data. Some problems were noticed along with the debris-covered glaciated area which was also difficult to identify with naked eye as it looked similar to the land surface.

The results presented indicate that SVM, ANN and RF are effective for mapping glacier and debris-covered glaciers from Sentinel-2 imagery data. Compared to the manual selection of segmentation parameters, these automatic methods for glacier map generation are more robust and highly accurate which will be helpful to determine the status of water resources more efficiently. The existing reference datasets have discrepancies and are not consistent with each other. In this context our highly accurate classification approach will be effective to develop a consistent and reliable glacier inventory dataset.

In future, we would like to integrate deep learning-based approach for automatic feature extraction using an unsupervised feature learning approach using autoencoder. It is expected that this will reduce the human efforts needed to prepare the hand-engineered features and it will help to improve the classification accuracy of the supervised classifiers for glacier mapping.

REFERENCES

[1] T. Yao, L. G. Thompson, V. Mosbrugger, F. Zhang, Y. Ma, T. Luo, B. Xu, X. Yang, D. R. Joswiak, W. Wang, M. E. Joswiak, L. P. Devkota, S. Tayal, R. Jilani, and R. Fayziev, "Third pole environment (TPE)," *Environ. Develop.*, vol. 3, pp. 52–64, Jul. 2012.

[2] J. Gardelle, E. Berthier, and Y. Arnaud, "Slight mass gain of Karakoram glaciers in the early twenty-first century," *Nature Geosci.*, vol. 5, no. 5, pp. 322–325, May 2012.

[3] A. A. Tahir, P. Chevallier, Y. Arnaud, L. Neppel, and B. Ahmad, "Modeling snowmelt-runoff under climate scenarios in the Hunza river basin, Karakoram range, Northern Pakistan," *J. Hydrol.*, vol. 409, nos. 1–2, pp. 104–117, Oct. 2011.

[4] A. A. Khan, S. N. ul Hassan, S. Baig, M. Z. Khan, and A. Muhammad, "The response of land surface temperature to the changing land-use land-cover in a mountainous landscape under the influence of urbanization: Gilgit city as a case study in the Hindu Kush himalayan region of Pakistan," *Int. J. Econ. Environ. Geol.*, vol. 10, no. 3, pp. 40–49, Dec. 2019. [Online]. Available: https://www.econ-environ-geol.org/index.php/ojs/article/view/307/221

[5] M. Aniya, P. Skvarca, H. Sato, R. Naruse, and G. Casassa, "The use of satellite and airborne imagery to inventory outlet glaciers of the southern Patagonia icefield, South America," *Photogramm. Eng. Remote Sens.*, vol. 62, no. 12, pp. 1361–1369, 1996.

[6] J. Gao and Y. Liu, "Applications of remote sensing, GIS and GPS in glaciology: A review," *Prog. Phys. Geogr.*, vol. 25, no. 4, pp. 520–540, Dec. 2001.

[7] N. R. Pal and S. K. Pal, "A review on image segmentation techniques," *Pattern Recognit.*, vol. 26, no. 9, pp. 1277–1294, 1993.

[8] F. Paul, C. Huggel, and A. Kääb, "Combining satellite multispectral image data and a digital elevation model for mapping debris-covered glaciers," *Remote Sens. Environ.*, vol. 89, no. 4, pp. 510–518, Feb. 2004.

[9] K. A. L. Bibi, A. A. Khan, G. Khan, "Snow cover trend analysis using modis snow products: A case of Shayok river basin in Northern Pakistan," *J. Himalayas Earth Sci.*, vol. 52, no. 2, pp. 145–160, 2019.

[10] R. Nijhawan, P. Garg, and P. Thakur, "A comparison of classification techniques for glacier change detection using multispectral images," *Perspect. Sci.*, vol. 8, pp. 377–380, Sep. 2016.

[11] H. Alifu, R. Tateishi, and B. Johnson, "A new band ratio technique for mapping debris-covered glaciers using landsat imagery and a digital elevation model," *Int. J. Remote Sens.*, vol. 36, no. 8, pp. 2063–2075, Apr. 2015.

[12] S. Gindraux, R. Boesch, and D. Farinotti, "Accuracy assessment of digital surface models from unmanned aerial vehicles' imagery on glaciers," *Remote Sens.*, vol. 9, no. 2, p. 186, Feb. 2017.

[13] A. A. Othman and R. Gloaguen, "Integration of spectral, spatial and morphometric data into lithological mapping: A comparison of different machine learning algorithms in the Kurdistan region, NE Iraq," *J. Asian Earth Sci.*, vol. 146, pp. 90–102, Sep. 2017.

[14] H. Frey, H. Machguth, M. Huss, C. Huggel, S. Bajracharya, T. Bolch, A. Kulkarni, A. Linsbauer, N. Salzmann, and M. Stoffel, "Estimating the volume of glaciers in the Himalayan–Karakoram region using different methods," *Cryosphere*, vol. 8, no. 6, pp. 2313–2333, Dec. 2014.

[15] M. Akhtar, N. Ahmad, and M. Booij, "The impact of climate change on the water resources of Hindukush–Karakorum–himalaya region under different glacier coverage scenarios," *J. Hydrol.*, vol. 355, nos. 1–4, pp. 148–163, Jun. 2008.

[16] M. Shrestha, T. Koike, Y. Hirabayashi, Y. Xue, L. Wang, G. Rasul, and B. Ahmad, "Integrated simulation of snow and glacier melt in water and energy balance-based, distributed hydrological modeling framework at Hunza river basin of Pakistan Karakoram region," *J. Geophys. Res. Atmos.*, vol. 120, no. 10, pp. 4889–4919, May 2015.

[17] C. Gul, S.-C. Kang, B. Ghauri, M. Haq, S. Muhammad, and S. Ali, "Using landsat images to monitor changes in the snow-covered area of selected glaciers in northern Pakistan," *J. Mountain Sci.*, vol. 14, no. 10, pp. 2013–2027, Oct. 2017.

[18] A. Khan, B. S. Naz, and L. C. Bowling, "Separating snow, clean and debris covered ice in the Upper Indus Basin, Hindukush-Karakoram-himalayas, using landsat images between 1998 and 2002," *J. Hydrol.*, vol. 521, pp. 46–64, Feb. 2015.

[19] L. Zhang, Q. Zhang, B. Du, X. Huang, Y. Y. Tang, and D. Tao, "Simultaneous spectral-spatial feature selection and extraction for hyperspectral images," *IEEE Trans. Cybern.*, vol. 48, no. 1, pp. 16–28, Jan. 2018.

[20] L. Zhang, L. Zhang, and B. Du, "Deep learning for remote sensing data: A technical tutorial on the state of the art," *IEEE Geosci. Remote Sens. Mag.*, vol. 4, no. 2, pp. 22–40, Jun. 2016.

[21] A. Jamil and B. Bayram, "Tree species extraction and land use/cover classification from high-resolution digital orthophoto maps," *IEEE J. Sel. Topics Appl. Earth Observ. Remote Sens.*, vol. 11, no. 1, pp. 89–94, Jan. 2018.

[22] Y. Qian, W. Zhou, J. Yan, W. Li, and L. Han, "Comparing machine learning classifiers for object-based land cover classification using very high resolution imagery," *Remote Sens.*, vol. 7, no. 1, pp. 153–168, Dec. 2014.

[23] A. Zarea and A. Mohammadzadeh, "A novel building and tree detection method from LiDAR data and aerial images," *IEEE J. Sel. Topics Appl. Earth Observ. Remote Sens.*, vol. 9, no. 5, pp. 1864–1875, May 2016.

[24] L. Zhang and J. You, "A spectral clustering based method for hyperspectral urban image," in *Proc. Joint Urban Remote Sens. Event (JURSE)*, Mar. 2017.

[25] Y. Wu, B. Jiang, and Y. Wang, "Incipient winding fault detection and diagnosis for squirrel-cage induction motors equipped on CRH trains," *ISA Trans.*, to be published.

[26] Y. Wu, B. Jiang, and N. Lu, "A descriptor system approach for estimation of incipient faults with application to high-speed railway traction devices," *IEEE Trans. Syst., Man, Cybern., Syst.*, vol. 49, no. 10, pp. 2108–2118, Oct. 2019.

[27] J. Zhang, L. Jia, M. Menenti, and G. Hu, "Glacier facies mapping using a machine-learning algorithm: The Parlung Zangbo basin case study," *Remote Sens.*, vol. 11, no. 4, p. 452, Feb. 2019.

[28] A. Pozdnoukhov, G. Matasci, M. Kanevski, and R. S. Purves, "Spatio-temporal avalanche forecasting with support vector machines," *Natural Hazards Earth Syst. Sci.*, vol. 11, no. 2, pp. 367–382, Feb. 2011.

[29] B. Feizizadeh, T. Blaschke, H. Nazmfar, E. Akbari, and H. R. Kohbanani, "Monitoring land surface temperature relationship to land use/land cover from satellite imagery in Maraqeh county, Iran," *J. Environ. Planning Manage.*, vol. 56, no. 9, pp. 1290–1315, Nov. 2013.

[30] G. Chander, B. L. Markham, and D. L. Helder, "Summary of current radiometric calibration coefficients for Landsat MSS, TM, ETM+, and EO-1 ALI sensors," *Remote Sens. Environ.*, vol. 113, no. 5, pp. 893–903, May 2009.

[31] T. G. Farr, "The shuttle radar topography mission," *Rev. Geophys.*, vol. 45, no. 2, May 2007, Art. no. RG2004.

[32] S. R. Bajracharya, S. B. Maharjan, F. Shrestha, W. Guo, S. Liu, W. Immerzeel, and B. Shrestha, "The glaciers of the Hindu Kush himalayas: Current status and observed changes from the 1980s to 2010," *Int. J. Water Resour. Develop.*, vol. 31, no. 2, pp. 161–173, Apr. 2015.

[33] S. R. Bajracharya, S. B. Maharjan, and F. Shrestha, "Glaciers in the Indus Basin," in *Indus River Basin*, S. I. Khan and T. E. Adams, Eds. Amsterdam, The Netherlands: Elsevier, 2019, ch. 5, pp. 123–144, doi: 10.1016/B978-0-12-812782-7.00006-0.

[34] P. Mohanaiah, P. Sathyanarayana, and L. Gurukumar, "Image texture feature extraction using GLCM approach," *Int. J. Sci. Res. Publication*, vol. 3, no. 1, pp. 2250–3153, 2013.

[35] R. M. Haralick, K. Shanmugam, and I. Dinstein, "Textural features for image classification," *IEEE Trans. Syst., Man, Cybern. Syst.*, vol. TSMC-3, no. 6, pp. 610–621, Nov. 1973.

[36] ESA. *SNAP|STEP*. Accessed: Jul. 7, 2019. [Online]. Available: https://step.esa.int/main/toolboxes/snap/

[37] M. Belgiu and L. Drăguţ, "Random forest in remote sensing: A review of applications and future directions," *ISPRS J. Photogram. Remote Sens.*, vol. 114, pp. 24–31, Apr. 2016.

[38] G. Omer, O. Mutanga, E. M. Abdel-Rahman, and E. Adam, "Performance of support vector machines and artificial neural network for mapping endangered tree species using worldview-2 data in Dukuduku forest, South Africa," *IEEE J. Sel. Topics Appl. Earth Observ. Remote Sens.*, vol. 8, no. 10, pp. 4825–4840, Oct. 2015.

[39] F. Melgani and L. Bruzzone, "Classification of hyperspectral remote sensing images with support vector machines," *IEEE Trans. Geosci. Remote Sens.*, vol. 42, no. 8, pp. 1778–1790, Aug. 2004.

[40] P. Ghamisi, J. Plaza, Y. Chen, J. Li, and A. Plaza, "Advanced supervised spectral classifiers for hyperspectral images: A review," *IEEE Geosci. Remote Sens. Mag.*, vol. 5, no. 1, pp. 8–32, Mar. 2017.

[41] P. O. Gislason, J. A. Benediktsson, and J. R. Sveinsson, "Random forests for land cover classification," *Pattern Recognit. Lett.*, vol. 27, no. 4, pp. 294–300, Mar. 2006.

AFTAB AHMED KHAN was born in Gilgit-Baltistan, Pakistan. He received the B.S. (equivalent) degree in information technology from Pir Mehr Ali Shah Arid Agriculture University, Rawalpindi, the M.Sc. degree from the Technical University of Berlin, Germany, and the Ph.D. degree in 3D geoinformatics (indoor navigation) from the Technical University Munich, Germany, in 2015.

From 2013 to 2015, he was a Research Associate with the Technical University of Munich. Since 2016, he has been an Assistant Professor with the Computer Science Department, Karakoram International University, Gilgit, Pakistan. He is the author of two book chapters and more than 10 peer-reviewed articles. His research interests include 3D geoinformatics and machine learning using earth science informatics.

AKHTAR JAMIL was born in Gilgit-Baltistan, Pakistan. He received the B.S. degree in computer science from the University of Karachi, Karachi, Pakistan, in 2008, the M.S. degree in computer software engineering from the National University of Sciences and Technology, Islamabad, Pakistan, in 2011, and the Ph.D. degree in GIS and remote sensing from the Department of Geomatics Engineering, Yildiz Technical University, Istanbul, Turkey, in 2018. From 2009 to 2010, he was a Research Assistant with the Department of Computer Software Engineering, Military College of Signals, Rawalpindi, Pakistan. Then, he moved to the COMSATS Institute of Information Technology, from 2011 to 2014, as a Lecturer. He has been the Deputy Head of the Department and an Assistant Professor with the Department of Computer Engineering, Istanbul Sabahattin Zaim University, Istanbul, since 2018. His research interests include pattern recognition, machine learning, and remote sensing.

DOSTDAR HUSSAIN was born in Gilgit-Baltistan, Pakistan. He received the M.Sc. degree (equivalent) in information technology from Quaid-i-Azam University Islamabad, Pakistan, and the M.S. degree in computer science from Linköping University, Sweden. He is currently pursuing the Ph.D. degree with National Cheng Kung University, Taiwan. He is currently a Lecturer with the Department of Computer Science, Karakoram International University, Gilgit, Pakistan. His research interests include geoinformatics and machine learning. He is author of six research publications and three conferences papers.

MURTAZA TAJ received the B.E. degree (Hons.) (information technology) in engineering from Hamdard University, Pakistan, in 2003, and the M.Sc. and Ph.D. degrees in electronic engineering and computer science from the Queen Mary University of London (QMUL), U.K., in 2005 and 2009, respectively. He is currently a Visiting Assistant Professor with the Lahore University of Management Sciences, Pakistan. His research interest includes object detection and tracking using multimodal sensors. He has served as a Reviewer for the IEEE Transactions on Circuits and Systems for Video Technology. He was also a Reviewer of International Workshop on Content-Based Multimedia Indexing. He has also served as the Electronic Media Chair for the IEEE International Conference on Advanced Video and Signal Based Surveillance (AVSS), in 2007.

GUL JABEEN was born in Gilgit-Baltistan, Pakistan. She received the B.Sc. degree in computer science from Karakoram International University, Gilgit, Pakistan, the M.S. degree in computer science from International Islamic University, Islamabad, and the Ph.D. degree from Tsinghua University, Beijing, China, in 2019. Her research interests include software and information security, and prediction modeling.

MUHAMMAD KAMRAN MALIK received the Ph.D. degree in computer science. He is currently an Assistant Professor with the Punjab University College of Information Technology (PUCIT), Punjab University, Lahore, Pakistan, in 2018. He has more than 15 years of teaching and development experience. He holds one U.S. patent. He has authored 30 journal and conference papers. He has provided consultancy to many multinational firms on his research areas. His research interests include natural language processing, machine learning, and data science.